



LOADING EFFECT OF HEMATITE ON MORPHOLOGY AND CONDUCTIVITY OF PPY/ α -Fe₂O₃ NANOCOMPOSITES

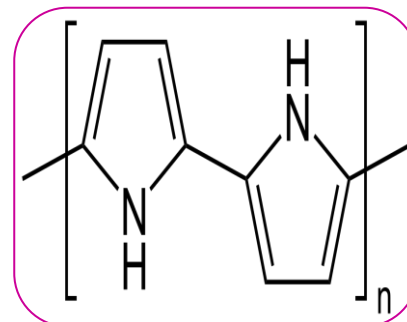
Tidke G. D.¹, Mahatme U. B.², Tabhane V. A.³, Utane Raju⁴.

¹ Nagar Parishad Jr. Science College, Kalmeshwar, Nagpur .

² Department of Physics, K. Z. S. Science College, Kalmeshwar .

³ Department of Physics, Pune University, Pune, India

⁴ Jijamata Jr. Science College, Butibori, Nagpur.



ABSTRACT

We prepared the conducting polymer (CP) polypyrrole (PPY) and its composites with α -Fe₂O₃ by in situ chemical oxidation polymerization using anhydrous FeCl₃ as oxidant and HCl as dopant by keeping different molar percentage of Fe₂O₃ with pyrrole monomer. The prepared PPY and PPY/ α -Fe₂O₃ composites were characterized by FTIR and UV-Vis spectroscopy and, their morphology examined by SEM and TEM techniques. The d.c. electrical conductivity (σ_{dc}) of PPY and nanocomposites (NCs) PPY/ α -Fe₂O₃ against temperature (32^oc – 100^oc) has been measure by four probe method.

KEYWORDS : Polypyrrole, Nanocomposites, FT-IR, UV-Vis, SEM, d.c. electrical conductivity .

I. INTRODUCTION:

There has been explosive growth of present era research in the field of CPs. With remarkable physical, thermal, electrical and magnetic properties, CPs have their potential application in various fields such as solar cell, light emitting diodes, sensors, molecular electronic devices, light weight batteries, biosensors, protecting agent and flexible displays [1].

So many efforts have been taken by researchers to change structure of CPs so that their applications should highly improve by using organic / inorganic dopants and oxidants [2]. Many investigated CPs are available but among these the PPY have high room temperature electrical conductivity, appreciable environmental stability, and easy synthesis, and easily doped with various dopants. Lot of potential application of PPY such as sensors, solid electrolytes and electrodes, for capacitor and solid state batteries have been reported [3].

Valuable ingredient Fe₂O₃ used in PPY/Fe₂O₃ composite which has been attractive physical and chemical properties such as low cost, non- toxicity, and, thermal and chemical stability. It has been identify as an important material used to modify biological active material, storage devices, magnetic sensors and catalysts [4].

The conducting polymer composite (CPC), PPY/Fe₂O₃ plays an important role due to physical and thermal stability, easy synthesis, facial processing, bio compatibility, reversibility and switching capacity and non-explosive. It is used in biosensors, chromatography, batteries and photovoltaic devices [5]. Wanchun Jiang et al (2016) reported the enhanced electromagnetic absorbing (EA) performance of α -Fe₂O₃/PPY (prepared by a facile one-step method) composite. Potential application for microwave absorption of this composite also has been reported [6].

In the present study, we report the preparation of PPY and PPY/ α -Fe₂O₃ composites via in situ chemical oxidation polymerization [7]. FTIR, UV-Visible and SEM techniques are used to investigate their characteristics, morphology and structural information. In this study we report the effect of different molar concentration of Fe₂O₃ in composites on the morphology, optical property and dc conductivity.

II. EXPERIMENTAL

A. Materials

Pyrrole monomer (AR grade Sigma-Aldrich) was purified by distillation under reduced pressure and stored at about 10 degree Celsius before use. The anhydrous FeCl₃ (AR grade), Hematite (α -Fe₂O₃) (AR grade) and HCl, all of MERCK make, are used in the present study. Deionized water was used as a solvent for all solutions.

B. Preparation of PPY

The PPY is synthesized by in-situ chemical oxidation method at room temperature (32°C). First oxidant solution of 16.2 gm (1M) anhydrous FeCl₃ in 100 ml deionized water was stirred for 1 hr. The second aqueous solution containing 3.45 ml (0.5M) pyrrole in 50 ml deionized water was stirred for 1 hr. Then after the first solution has been added drop wise in second aqueous solution of PPY and stirred for 6 hrs [8]. The prepared greenish black colored solution was filtered, then washed by distilled water and methanol till getting colorless filtrate. Resulting greenish black precipitate was dried at 60°C up to 8 hrs. On the basis of characterization resulting precipitate was identified as PPY [9,10].

C. Preparation of PPY/Fe₂O₃ composites

The first 50 ml aqueous solution containing 3.45 ml (0.5M) pyrrole was stirred for 1 hr. The second 100 ml aqueous solution containing different weight percent of Fe₂O₃ (15% to 30 %) with monomer (0.075M, 0.1M, 0.125M, 0.15M) [11] and 1.225 ml (0.4M) HCl was stirred for 1 hr. Third 100 ml aqueous solution of 1M FeCl₃ (16.2 gm) and 1M H₂SO₄ (5.389 ml) was stirred for 1 hr. Second and third solutions were mixed and stirred for 20 minutes. Then first solution added drop wise in it and stirred for 6 hrs. The resulting precipitates (changing color from brown to greenish black) [12,13] were filtered and washed with deionized water and methanol till getting colorless filtrate. Resulting precipitates were dried at 60°C for 8 hrs. [14].

D. Pellets designing

The samples of PPY and PPY/ α -Fe₂O₃ so obtained were crushed and finely ground using mortar and pestle to make fine powder. The pellets of thickness 3 to 4 mm were designed in die-punch (13 mm diameter) using hydraulic press at the pressure of 15 tons.

E. Measurement and characterization techniques

All samples were characterized by FTIR and UV-vis spectroscopy. Their morphological and structural study has been done by SEM technique. Four probe set up (DFP-RM -SES Roorkee - India) was used to examine dc electrical conductivity of all sample pellets. The discussion in detail regarding the results of FTIR, UV-vis spectroscopy (IIIA, IIIB), SEM (III C) and dc conductivity (III D) has been given in the following part III.

III. RESULT and DISCUSSION

A. FTIR spectra

FTIR spectra (Fig.1) of PPY and PPY/ α -Fe₂O₃ composites are enriched with absorption peaks attributes the typical characteristics of PPY which are in the range of 4000-500 cm⁻¹ consistent with literature. Figure 1(a) shows a typical FTIR spectrum of PPY granules. The peaks at 3434.34 cm⁻¹ attribute to free N-H stretching vibration mode of secondary amines having aromatic structure. The peaks at 1543.31 cm⁻¹ and 1452.30 cm⁻¹ corresponds to the stretching vibration of C=C and the C-C of PPY respectively. The band of C-N and C-H in plane deformation vibration are located at 1174.42 cm⁻¹ while the band of =C-H out of plane deformation vibration indicating polymerization of pyrrole at 910.74 cm⁻¹. The strong absorption bands in the region 805–1591 cm⁻¹ are corresponds to the characteristics of PPY [15].

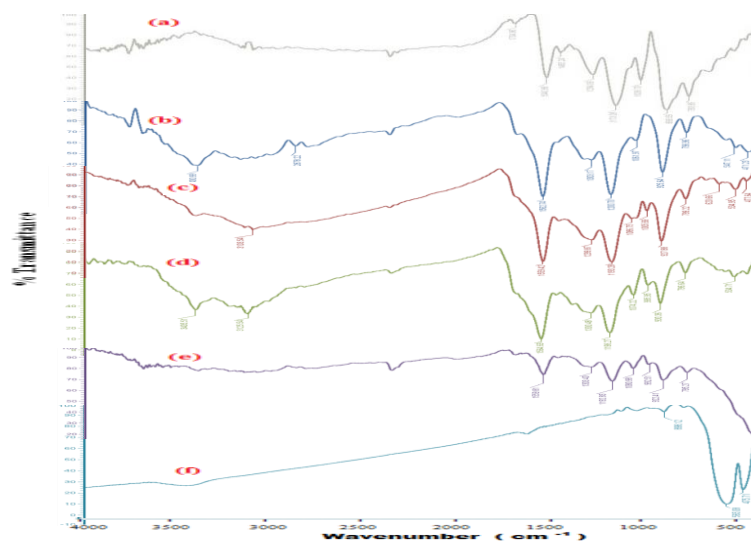


Figure 1: FTIR spectra of (a) Pure PPY, (b) PPY/15% α -Fe₂O₃, (c) PPY/20% α -Fe₂O₃, (d) PPY/25% α -Fe₂O₃ (e) PPY/30% Fe₂O₃ & (f) α -Fe₂O₃

Figure 1(f) shows IR spectra of α -Fe₂O₃ with a characteristic IR peak being observed at 565.08 cm⁻¹ could be assigned to M-O lattice vibration. The band at 898.12 cm⁻¹ is assigned to the Fe-O-Fe bending vibration [16].

Figure 1(b-1e) shows FTIR spectra of PPY/ α -Fe₂O₃ composites. In case of PPY/ 20% α -Fe₂O₃, the peak at 3405.21 cm⁻¹ and 3125.54 cm⁻¹ attribute to N-H stretching vibration mode of secondary amines and =CH-H alkene respectively. The peak at 1300.48 cm⁻¹ is due to fundamental vibration of PPY ring. The peak at 1564.69 cm⁻¹ attribute to C=C stretching. The peak at 1074.22 cm⁻¹ refers C-H in plane bend and peak at 1198.27 cm⁻¹ corresponds to ring breathing. In addition to these peaks two peaks are noticed at 930.36 cm⁻¹ and 796.64 cm⁻¹ in nanocomposite (NC) which assigned to the O-H bend and C-H out of plane deformation [17]. The peaks match well with the previous studies. It is clear from FTIR spectra that NCs have almost identical peaks those associated with pure PPY. With α -Fe₂O₃ loading in NCs, the identity peaks of PPY for bonds C=C, C-N, C-H and =C-H shows alternate red and blue shifts with increasing wt% of Fe₂O₃ in the NCs. Identity peak of C-C bond on PPY IR spectra suppressed in the NCs with the loading of Fe₂O₃. Thus we ensure the better intercalation of Fe₂O₃ with PPY in the NCs.

B. UV- Visible spectra:

Each of spectra reveals the presence of two absorption bands: one in the visible region and another in the UV region. For pure PPY (Figure 2 a) the band in the UV region at 357 nm having an absorption of 1.501 corresponds to the π - π^* transition and the band in the visible region at 533 nm having an absorption of 1.4349 corresponds to the n - π^* transition. The band in the visible region corresponds to their ring charge transfer associated with benzenoid to quinoid (interchain) moieties for PPY [18].

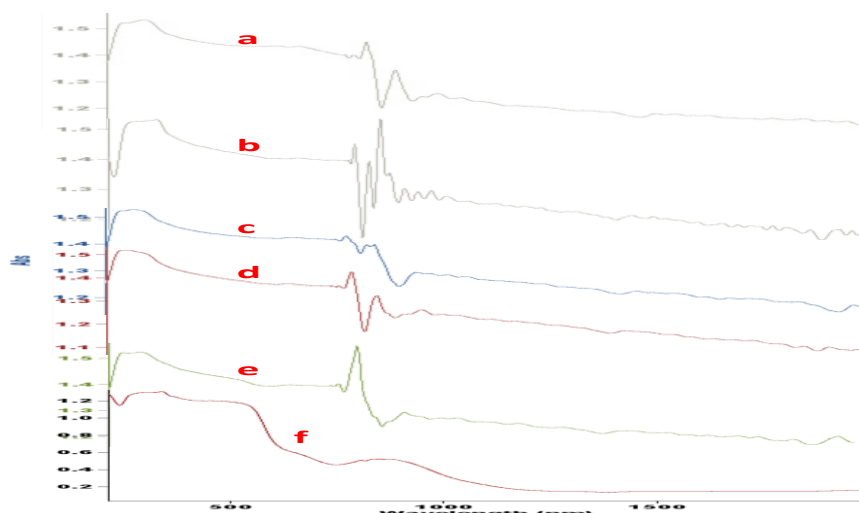


Figure 2: UV-Vis spectra of (a) Pure PPY, (b) PPY/15% α -Fe₂O₃, (c) PPY/20% α -Fe₂O₃, (d) PPY/25% α -Fe₂O₃, (e) PPY/30% Fe₂O₃ & (f) α -Fe₂O₃

Figure 2 (f), UV-vis spectra of α -Fe₂O₃, shows the absorption peaks at 363 nm (UV region) and 747 nm (visible region) having 1.3241 and 0.5273 absorbance respectively. The purchased Fe₂O₃ is of hematite (α -nature) has been supported by reported data [19,20]

Figure 2 (b-e), spectra for PPY/ α -Fe₂O₃ NCs, shows the peaks at 336 nm and 787 nm for PPY/ 15% α -Fe₂O₃, assigns π - π^* transition (intrachain transitions in benzenoid ring) and n - π^* transition (interchain hopping from benzenoid to quinoid – HOMO to LUMO or exciton absorption in quinoid rings -) with absorbances 1.533 and 1.451 respectively. It shows good agreement for conjugated polymer chain in PPY/ α -Fe₂O₃ NCs. Shift in λ_{\max} value for most of composite samples due to their structural changes arises due to loading of Fe₂O₃ [21,22]. With increasing wt% of Fe₂O₃ in the NCs, the absorption peaks in the UV region shows blue shift up to 25% loading of Fe₂O₃ and again shows red shift for further loading up to 30%. Alternate blue and red shifts are observed in the visible region for increasing weight percent of Fe₂O₃ in NCs. It reveals the better agreement for the agglomeration between PPY and Fe₂O₃. UV-vis absorbance data and band energy (eV) of PPY, α -Fe₂O₃ and PPY/ α -Fe₂O₃ NCs are given in table 1. The calculated values of transition band energy and exciton band energies of PPY are 3.801 eV and 1.612 eV respectively. The band energies of NCs are found to be lowered than PPY for 15% wt of Fe₂O₃ in NCs. With rise in wt% of Fe₂O₃ in NCs, the transition band energy has found to be increases up to 25% wt of Fe₂O₃ and decreases for further addition of Fe₂O₃ in NCs. With rise in wt% of Fe₂O₃ in NCs, the exciton band energy has found to be increased.

Table: 1 – UV-Vis absorbance data and band energy of PPY, α -Fe ₂ O ₃ and PPY/ α -Fe ₂ O ₃ NCs						
Samples	λ_{\max} (nm)		Absorbance		Band energy (eV)	
	π - π^*	n - π^*	π - π^*	n - π^*	π - π^*	n - π^*
	Transition Band	Exciton Band	Transition Band	Exciton Band	Transition Band	Exciton Band
PPY	327	771	1.534	1.401	3.801	1.612
α -Fe ₂ O ₃	340	849	1.31	0.525	3.656	1.464
PPY/ 15% α -Fe ₂ O ₃	336	787	1.533	1.451	3.699	1.579
PPY/ 20% α -	309	778	1.528	1.43	4.023	1.597

Fe ₂ O ₃						
PPY/ 25% α -Fe ₂ O ₃	282	800	1.518	1.426	4.408	1.553
PPY/ 30% α -Fe ₂ O ₃	320	773	1.524	1.403	3.884	1.608

SCANNING ELECTRON MICROSCOPE (SEM) ANALYSIS

SEM technology has used to analyze the size and shape of present CP, additive and NCs. Figure 3 (a), SEM image of PPY shows the granule clusters having spherical morphology with 211 nm in average diameter. Formation of smooth and homogeneous PPY granules can be clearly seen [23].

Figure 3 (b-e), SEM images of PPY/ α -Fe₂O₃ NCs shows the Fe₂O₃ nanoparticles are covered by spherical granules of PPY and forms multiple aggregation because of weak interparticle interaction. It shows the presence of spherical particle cluster of polymer in the composite which reveals the presence of Fe₂O₃ in PPY. The average size of PPY/ α -Fe₂O₃ NCs is about 107 nm and gives small decrease in granule size by adding the wt% of Fe₂O₃[24].

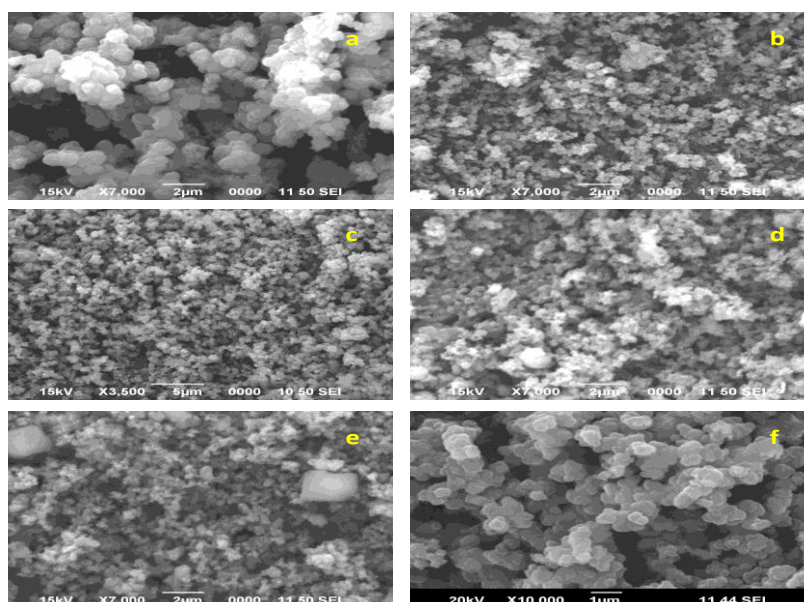


Figure 3: UV-vis spectra of (a) Pure PPY, (b) PPY/15% α -Fe₂O₃, (c) PPY/20% α -Fe₂O₃, (d) PPY/25% α -Fe₂O₃ (e) PPY/30% Fe₂O₃ & (f) α -Fe₂O₃

M.M. Rahman Khan et al (2012) reported the loading effect of CuO on the morphology and diameter of PANI/CuO nanofibers (NFs). Smallest diameter of NFs has been reported for the lowest loading of CuO in NFs. The loading of appropriate amount of metal oxides can be directly control the particle size of CPCs [25]. Thus, the addition of CuO always gave NFs with regular and uniform surface morphology whether the loadings of CuO is lower or higher.

Continuous increase in the volume of the core shell in PANI/TiO₂ composites with increase in percentage of nanocrystalline TiO₂ in polyaniline matrix has reported by Ameena Parveen et al (2013) [26]. The composite particles are clustered, homogeneous and circular in shape and have almost similar in size.

Similar size control of CPC by the loading of metal oxide has been observed in the present study, but the smallest particle size of CPC is for lowest wt% (15%) and highest wt% (30%) of metal oxide Fe₂O₃ in NCs. Overall, no much change in particle size has observed with loading of Fe₂O₃ but the composite particles are clustered, homogeneous and nearly spherical in shape and have almost similar in size.

C. ELECTRICAL DC CONDUCTIVITY

Fig. 4 displays the temperature dependence of the DC conductivity of samples of PPY and NCs. The dc surface conductivity measurements of the pure PPY and PPY/ α -Fe₂O₃ NCs were observed with decreasing temperature from 368 K to 298 K. It was observed that the electrical conductivity of the sample increases with increase in temperature and the values were in the order of 10^{-1} to 10^0 S cm⁻¹ for PPY composites whereas 10^0 S cm⁻¹ for PPY/ α -Fe₂O₃ which lies in the semi-conductor region [27] and they followed the Arrhenius equation similar to other semiconductors. Conductivity of NCs increases with increasing molar concentration of Fe₂O₃ up to 25% wt. mole may be due to a high polarization rate [28]. For further increase in molar weight of Fe₂O₃ up to 30% the dc conductivity of NCs decreases. The decrease in conductivity at 30% wt of metal oxide is may be due to low polarization rate. The change in dc conductivity of CPCs with metal oxides additive wt% has been reported in our previous study [29].

Conductivity of PPY and its NCs increases with increase in temperature. It may be due to a hopping mechanism between coordinating sides, local structural relaxations, segmental motions and thus overall "thermal activated behavior", following (VRH model) [30, 31, 32] Mott's equation

$$\sigma = \sigma_0 \exp \left[- \left(T_0 / T \right)^{1/n+1} \right], n=1,2,3 \quad \text{----- (1)}$$

Where, σ is the conductivity of the sample at temperature T (K), σ_0 is the pre-exponential factor (S/cm), T_0 is the characteristic Mott temperature (K) and $n = 3, 2, 1$ have to use for three, two and one dimensional nanosystems respectively. In our present study, as the samples are of three dimensional structure, we have to use $n = 3$.

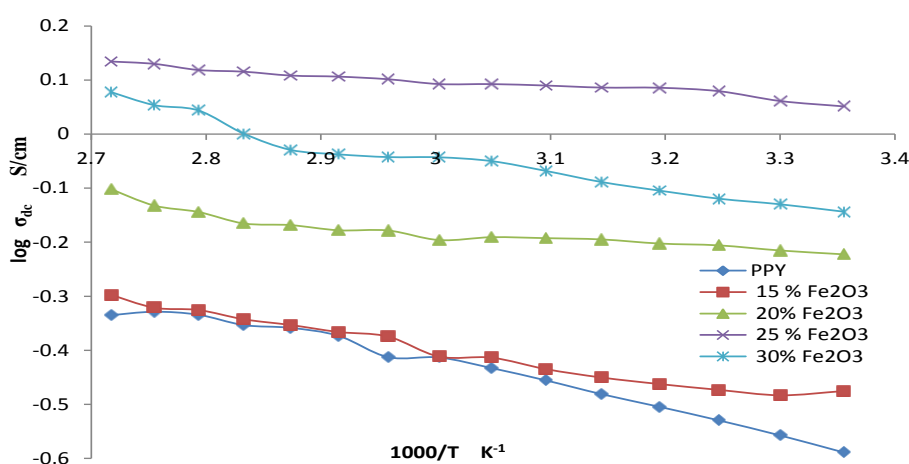


Figure 4: Electrical conductivity σ_{dc} of (a) Pure PPY, (b-e) PPY/15% α -Fe₂O₃

IV. CONCLUSION

The PPY and composites PPY/ α -Fe₂O₃ have been successfully synthesized using Chemical Oxidation Method. The FTIR spectra peaks of PPY and PPY/ α -Fe₂O₃ composite with different molar percent of α -Fe₂O₃ shows formation of CP and NCs using pyrrole monomer. FTIR of composites shows presence of metal oxide and it involve chemically in PPY. UV-Vis spectra show formation of absorption band in both UV and Visible region, and exhibited a good support with the conductivity result. SEM image shows granular surface morphology of PPY. SEM images of PPY/ α -Fe₂O₃ NCs also shows its homogeneous granular distribution (nearly spherical) of decreasing particle size with increasing molar percent of α -Fe₂O₃. Electrical conductivity σ (dc) decreases with decreasing temperature. The average surface dc conductivity of PPY at room

temperature is 0.4128 S/cm and dc conductivity of NCs increases with increase in molar concentration of Fe_2O_3 in composites.

ACKNOWLEDGEMENTS

The authors are very grateful to Sophisticated Analytical Instrumentation Center (STIC), Cochin for providing laboratory characterization facility and to Prof. Dattatraya Late of N.C.L. Pune, India, for his valuable guidance.

REFERENCES

- [1] Hongbo Gu, Jiang Guo, Xingru Yan, Huige Wei, Xi Zhang, Jiurong Liu, Yudong Huang, Suying Wei, Zhanhu Guo, "Electrical transport and magnetoresistance in advanced polyaniline nanostructures and nanocomposites", *Polymer*, 55(17), 4405–4419. doi.org/10.1016/j.polymer.2014.05.024 0032
- [2] Mansoor Farbod, Somayeh Khajepour, Ahvaz Iran, "Electrical properties and glass transition temperature of multiwalled carbon nanotube/polyaniline composites", *Journal of Non-Crystalline Solids*, 358(11), 1339–1344. doi: 10.1016/j.jnoncrysol.2012.03.006
- [3] Hesam Ghasemi, Uttandaraman Sundararaj, "Electrical properties of in situ polymerized polystyrene/polyaniline composites: The effect of feeding ratio", *Synthetic Metals*, 162(13–14), 1177–1183. doi.org/10.1016/j.synthmet.2012.04.037.
- [4] S. A. Nabz, Mohammad Shahadat, Rani Bushra, M. Oves, Faheem Ahmed, "Synthesis and characterization of polyaniline/Zr(IV) sulphosalicylate composite and its applications" (1) electrical conductivity, and (2) antimicrobial activity studies, *Chemical Engineering Journal* 173 (2011) 706–714 doi:10.1016/j.cej.2011.07.081
- [5] Anode Tae Hwan Lim, Kyung Wha Oh, Seong Hun Kim "Self-assembly supramolecules to enhance electrical conductivity of polyaniline for a flexible organic solar cells", *Solar Energy Materials and Solar Cells*, 101, 232–240. doi:10.1016/j.solmat.2012.01.040
- [6] Wanchun Jiang, Mengxiao Sun, Kun Zhang, Fan Wu, Aming Xie, and Mingyang Wang, "Three-dimensional (3D) α - Fe_2O_3 /polypyrrole (PPy) nanocomposite for effective electromagnetic absorption", *AIP ADVANCES* 6, 065021 (2016). doi.org/10.1063/1.4954932
- [7] Kaur, G., Adhikari, R., Cass, P., Bown, M., & Gunatillake, P., "Electrically conductive polymers and composites for biomedical applications", *RSC Advances*, 5, 37553–37567. doi.org/10.1039/C5RA01851J
- [8] A. Muñoz-Bonilla, J. Sánchez-Marcos and P. Herrasti, "Magnetic Nanoparticles-Based Conducting Polymer Nanocomposites", *AIP Advances*. 2016. doi: 10.1007/978-3-319-46458-9-2
- [9] Bai-Huan Xu, Bi-Zhou Lin, Zhi-Jian Chen, Xiao-Li Li, Qin-Qin Wang, "Preparation and electrical conductivity of polypyrrole/ WS_2 layered nanocomposites", *Science*, 330(1), 220–226, Elsevier Inc. doi:10.1016/j.jcis.2008.10.033
- [10] M. D. Migahed, T. Fahmy, M. Ishra, A. Barakat, "Preparation, characterization, and electrical conductivity of polypyrrole composite films", *Polymer Testing*, 23(3), 361–365. doi: 10.1016/j.carbpol.2010.05.036
- [11] Chao Yang, Tingmei Wang, Peng Liu, Huigang Shi, Desheng Xue, "Preparation of well-defined blackberry-like polypyrrole/fly ash composite microspheres and their electrical conductivity and magnetic properties matter", *Current Opinion in Solid State and Materials Science*, 13(5–6), 112–118. 2009, Elsevier Ltd. doi: 10.1016/j.cossms.2009.06.002
- [12] Saswata Bose, Ananta Kumar Mishra, Tapas Kuila, Nam Hoon Kim, Ok-Kyung Park, JoongHee, "Tunable electrical conductivity and dielectric properties of triglycine sulfate-polypyrrole composite matter", *Chemical Engineering Journal*, 187, 334–340, 2012 Elsevier doi: 10.1016/j.cej.2012.01.081
- [13] Rodica Plugaru, Titus Sandu, Neculai Plugaru, "First principles study and variable range hopping

- conductivity in disordered Al/Ti/Mn-doped ZnO", *RESULTS IN PHYSICS*, (2012), 2, 190–197, Elsevier B.V. doi.org/10.1016/j.rinp.2012.10.004
- [14] Hosford J., Valles M., Krainer F. W., Glieder A., & Wong, L. S., "Parallelized biocatalytic scanning probe lithography for the additive fabrication of conjugated polymer structures" *Nanoscale*, (2018), 10(15), 7185–7193. doi.org/10.1039/c8nr01283k
- [15] Khan A. A., & Paquiza L., "Electrical behavior of conducting polymer based 'polymeric –inorganic' nanocomposite: Polyaniline and polypyrrole zirconium titanium phosphate", *Synthetic Metals*, (2011), 161(9–10), 899–905. doi.org/10.1016/j.synthmet.2011.02.022
- [16] Irina Sapurina, Yu Li, Elizaveta Alekseeva, Patrycja Boberet all, "Polypyrrole nanotubes: The tuning of morphology and conductivity", *Polymer* 113 (2017) 247-258 doi.org/10.1016/j.polymer.2017.02.064
- [17] V. S. Shanthala, S. N. Shobha, Devi, M. V. Murugendrappa, "Synthesis characterization and DC conductivity studies of polypyrrole/copper zinc iron oxide nanocomposites", *J. Asian Ceramic Societies* 5 (2017) 227–234. doi.org/10.1016/j.jascer.2017.02.005
- [18] Nela Maráková, Petr Humpolíček et al., "Antimicrobial activity and cytotoxicity of cotton fabric coated with conducting polymers, polyaniline or polypyrrole, and with deposited silver nanoparticles", *Applied Surface Science* (2017). 396, 169–176. doi.org/10.1016/j.apsusc.2016.11.024
- [19] Lidia Armelaoy, Marco Bettinelliz, Maurizio Casariny, Gaetano Granozziy, Eugenio Tondelloy and Andrea Vittadini, "A theoretical and experimental investigation of the electronic structure of α -Fe₂O₃ thin films", *J. Phys.: Condens. Matter* 7 (1995) L299–L305.
- [20] Samira Bagheri, Chandrappa K. G. and Sharifah Bee Abd Hamid, "Generation of Hematite Nanoparticles via Sol-Gel Method", *Res. J. Chem. Sci.* Vol. 3(7), 62-68, July (2013), ISSN 2231-606X, ISCA.
- [21] Liu P., Wu S., Zhang Y., Zhang H., & Qin X., "A Fast Response Ammonia Sensor Based on Coaxial PPy– PANI Nanofiber Yarn", *Nanomaterials* **2016**, 6, 121; doi:10.3390/nano6070121
- [22] Mahatme U. B., S. P. Dongre, S. D. Thakre and A. A. Dani, "Additive weight percent dependence morphology of conducting polymer/metal oxide nanocomposites", *IJBAT*, 2 (1), 2014, PP 635-643 ISSN No.–2347-517X, ICAAMSD – 2014.
- [23] Kang K. S., Jee C. H., Bae J., Jung H. J., Huh P., Kang K. S., Jung H. J., "Synthesis and characterization of novel polypyrrole hybrid nanotubules incorporated with polyaniline spots", *AIP ADVANCES* **7**, 115219 (2017) 115219-1-5. <https://doi.org/10.1063/1.4985689>
- [24] AS Silva, SM de Souza and EA Sanches, "Polypyrrole @ α -Al₂O₃ and polypyrrole @ CeO₂ core-shell hybrid nanocomposites", *Journal of Composite Materials* (2017) 0(0)1–9 doi: 10.1177/0021998317725908
- [25] Mohammad Mizanur Rahman Khana,, Yee Keat Wee, Wan Ahmad Kamil Mahmood, "Effects of CuO on the morphology and conducting properties of PANI nanofibers", *Synthetic Metals* 162 (2012) 1065– 1072. doi.org/10.1016/j.synthmet.2012.05.009
- [26] Ameena Parveen, Aashis S. Roy, "Effect of morphology on thermal stability of core-shell polyaniline/TiO₂ nanocomposites", *Adv. Mat. Lett.* 2013, 4(9), 696-701, doi: 10.5185/amlett.2012.12481
- [27] Shanthala, V. S., Devi, S. N. S., & Murugendrappa, M. V., "Journal of Asian Ceramic Societies Synthesis, characterization and DC conductivity studies of polypyrrole / copper zinc iron oxide nanocomposites", *Integrative Medicine Research*, (2017), 5(3), 227–234. doi.org/10.1016/j.jascer.2017.02.005
- [28] Abdulla, H. S., & Abbo, A. I., "Optical and Electrical Properties of Thin Films of Polyaniline and Polypyrrole", *Int. J. Electrochem. Sci.*, **7** (2012) 10666 - 10678.
- [29] S. D. Thakre, Mahatme U. B., A. A. Dani, "Preparation and Characterization of Polyaniline/Zinc Oxide Composites via Oxidative Polymerization", *International Journal of Composite Materials* 2014, 4(1) : 14-20. doi: 10.5923/j.cmaterials.20140401.03

[30] Hongbo Gu, Jiang Guo, Xingru Yan, Huige Wei, Xi Zhang, Jiurong Liu, Yudong Huang, Suying Wei, Zhanhu Guo, "Electrical transport and magnetoresistance in advanced polyaniline nanostructures and nanocomposites", *Polymer* 55 (2014) 4405 – 4419.

doi.org/10.1016/j.polymer.2014.05.024

[31] Gu H, Wei H, Guo J, Haldolaarachige N, Young DP, Wei S, et al., "Hexavalent chromium synthesized polyaniline nanostructures: Magnetoresistance and electrochemical energy storage behaviors" *Polymer* 2013;54:5974-5985.

doi.org/10.1016/j.polymer.2013.08.020

[32] Hongbo Gu, Jiang Guo, Huige Wei, Xi Zhang, Jiahua Zhu, Lu Shao, Yudong Huang, Neel Haldolaarachchige, David P. Young, Suying Wei, Zhanhu Guo, "Magnetoresistive conductive polymer-tungsten trioxide nanocomposites with ultrahigh sensitivity at low magnetic field", *Polymer* 55 (2014) 944-950. doi.org/10.1016/j.polymer.2013.12.024